

## Micro-laser assisted single point diamond turning of advanced optical materials

Robert Turnbull<sup>1</sup>, Jayesh Navare<sup>1</sup>, Sai Kode<sup>1</sup>, Stefan Krämer<sup>1,2</sup>

<sup>1</sup>Micro-LAM, Inc., 5960 S Sprinkle Rd, Portage, Michigan 49002, United States

<sup>2</sup>M10 Edge Ltd., Unit B, Argyle Gate, Argyle Way, Stevenage SG1 2AD, United Kingdom

[saikumar.kode@micro-lam.com](mailto:saikumar.kode@micro-lam.com)

### Abstract

This paper investigates the feasibility of single point diamond turning (SPDT) of advanced optical materials like silicon carbide, tungsten carbide, and fused silica glass, using the micro-laser assisted machining ( $\mu$ -LAM) process. It is observed that the machining dynamics, including selection of spindle speeds, linear feed rate, laser power, and depth of cut, is crucial for ductile material removal of these materials. While machining of tungsten carbide, spindle speed of 2000 RPM, linear feed of 1  $\mu$ m/rev, laser power output of 7.5 W, and depth of cut of 2  $\mu$ m resulted in surface roughness values of 3 nm to 5 nm RMS whereas during machining of silicon carbide, spindle speed of 375 RPM, linear feed of 0.4  $\mu$ m/rev, laser power output of 12 W, and depth of cut of 4  $\mu$ m resulted in surface roughness value of 10 nm RMS. It is also shown that an optimal tooling geometry with a steep negative rake of  $-65^\circ$  and 1.5 mm nose radius is capable of machining fused silica glass over commercially viable cutting distance and has surface roughness values of 20 nm to 30 nm and form irregularity of 0.5  $\mu$ m to 0.7  $\mu$ m PV.

Keywords : SPDT, UPM, SiC, fused silica, tungsten carbide

### 1. Introduction

Ultraprecision single point diamond turning has enabled the manufacturing of complex aspherical and freeform lenses using single crystal diamond cutting tools. This process is highly deterministic and cost effective when compared to its traditional counterparts such as grinding and polishing. However, SPDT of hard and brittle materials such as glass and ceramics poses a significant challenge from increased rate of tool wear and shorter cutting distances. The process of injection moulding for mass manufacturing of optical lenses where optical quality moulds made of tungsten carbide and silicon carbide are used has gained widespread traction due to their superior mechanical properties and resistance to wear. Material processing of such moulds is done using grinding and polishing as these processes are well established [1-3]. However, processing of moulds with complex miniature features using grinding is difficult due to geometry restrictions of the grinding wheel. Likewise, polishing miniature features has the same constraints with the lap size. SPDT, conversely, is a viable alternative for machining such features as the diamond cutting tools used can have extremely small nose radii from 10  $\mu$ m to 100  $\mu$ m.

Limited studies of applying SPDT to glass and ceramics have been published in the past. Mishra, *et al.*[4] have demonstrated SPDT of tungsten carbide mould material followed by chemical mechanical polishing for mass manufacturing of smartphone lens application. Li, *et al.* [5] have reported nano-scale surface roughness on tungsten carbide using ultrasonic assisted SPDT. But there is significant tool wear observed in the form of micro-chipping and abrasive wear. Thus, processing such mould materials in a commercially viable volume is a challenge. We propose investigating the feasibility of machining these materials using the micro-laser assisted diamond turning process ( $\mu$ -LAM). The objective of this study is to evaluate the machining of tungsten carbide, silicon carbide, and glass

workpieces and to answer three key questions: 1) what is the surface roughness of the workpiece machined with the  $\mu$ -LAM process?; 2) what is the form error induced during machining?; and 3) what is the usable cutting distance?

### 2. Micro-laser assisted diamond turning ( $\mu$ -LAM) process

Micro-laser assisted diamond turning process ( $\mu$ -LAM) consists of a 1064 nm wavelength Nd:YAG laser beam which is passed through a polished optical surface on the back face of a diamond cutting tool during SDPT. The geometry of this diamond cutting tool is defined such that laser beam is emitted at the cutting interface between the tool and the workpiece to facilitate ductile material removal. Details about this process can be found elsewhere[6]. Figure 1 shows a schematic of the  $\mu$ -LAM process.

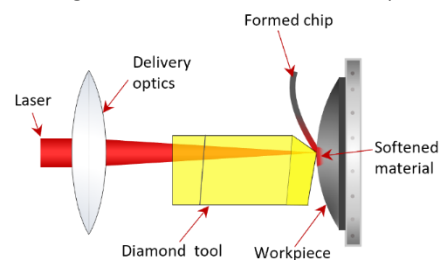


**Figure 1.** Schematic of  $\mu$ -LAM process. A laser is focused through the diamond tool to interact with the tool workpiece.

### 3. Experimental Method

#### 3.1. Testing plan and lab equipment

To investigate the feasibility of SPDT of tungsten carbide mould, a  $\varnothing$  5.4 mm tungsten carbide mould with a convex radius of curvature of 5 mm was machined on a diamond turning lathe. The silicon carbide machined was a  $\varnothing$  25 mm flat. The fused silica glass that was machined was a plano-convex lens with a radius of curvature of 34.39 mm and a diameter of 25 mm. The Optimus

T2, a micro-laser assisted toolpost depicted in Figure 2, was used to deliver a 1064 nm wavelength Nd:YAG laser beam at the cutting interface. The toolpost comprises of a tool holder, laser collimator, and a series of optical elements that direct the laser beam towards the cutting edge. The collimator was affixed to three linear stages that facilitate proper alignment of the laser in vertical, lateral, and axial (focus) direction with respect to the diamond tool. The laser beam is continuous and can be adjusted by 1 W power increments with maximum power output of 50 W.

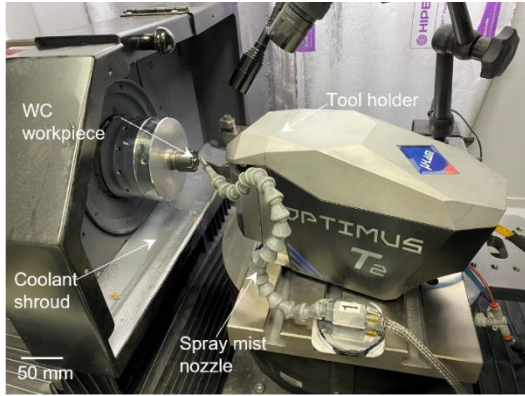


**Figure 2.** Experimental setup for cutting WC on a Precitech Nanoform X ultraprecision lathe. The Optimus T2 delivers the laser while simultaneously cutting the workpiece with a diamond tool.

### 3.2. Tungsten carbide workpiece machining

These tests were performed on a 4-axis Precitech Nanoform X ultraprecision lathe. Two tests were implemented in which a tungsten carbide mould was machined until the surface exhibited signs of tool failure during each test. This was assessed by setting a threshold value of 10 nm for RMS roughness. If the surface finish exceeded the threshold value, then the test was concluded and the total cutting distance covered by the tool before it exhibited failure was noted for each test. Same tungsten carbide mould was used in both the tests. To ensure similar starting conditions, *i.e.* fracture free surface for both tests, the mould was roughed using a separate roughing tool. Diamond tools manufactured by M10 Edge Ltd. were used for these tests and the finishing tools used for the tests had a geometry of  $-35^\circ$  rake,  $15^\circ$  clearance, and  $100\ \mu\text{m}$  nose radius. Smaller radii tools were selected as this geometry is typically required for machining intricate features on moulds used for manufacturing smartphone lenses. Machining parameters listed in Table 1 were used for both the tests.

**Table 1** Machining parameters for tungsten carbide mould

Process	RPM	Feed (mm/min)	Depth of cut ( $\mu\text{m}$ )	Power (W)	Coolant
Rough	2000	6	4	7.5	OMS
Finish	2000	2	2	7.5	OMS

### 3.3. Silicon carbide workpiece machining

These tests were performed on a 4-axis Precitech Nanoform X ultraprecision lathe operating with only two axes. Five tests were implemented in which a silicon carbide flat was machined until the surface exhibited signs of tool failure. This was assessed by setting a threshold value of 50 nm for RMS roughness. If the surface finish exceeded the threshold value then the test was concluded. Natural diamond tools manufactured by M10 Edge Ltd. were used for these tests and had a geometry of  $-25^\circ$  rake,  $10^\circ$  clearance, and 1.5 mm nose radius. Machining parameters listed in Table 2 were used for all the tests.

**Table 2** Machining parameters for silicon carbide

Test No.	RPM	Feed (mm/min)	Depth of cut ( $\mu\text{m}$ )	Power (W)	Coolant
1	375	1.25	4	6	OMS
2	375	0.6	4	6	OMS
3	375	0.3	4	6	OMS
4	375	0.3	4	12	OMS
5	375	0.15	4	12	OMS

### 3.4. Fused silica workpiece machining

These tests were performed on a 3-axis Nanotech 250 UPL ultraprecision lathe operating with only two axes. Three tests were implemented in which a fused silica convex lens was machined until the surface exhibited signs of tool failure. This was assessed by setting a threshold value of 50 nm for RMS roughness. If the surface finish exceeded the threshold value then the test was concluded. Synthetic diamond tools manufactured by M10 Edge Ltd. were used for these tests and had a geometry of  $-65^\circ$  rake,  $10^\circ$  clearance, and 1.5 mm nose radius. Machining parameters listed in Table 3 were used for all the tests.

**Table 3** Fused silica machining parameters

Test No.	RPM	Feed (mm/min)	Depth of cut ( $\mu\text{m}$ )	Power (W)	Coolant
1	1000	1	6	7	316-HT
2	4000	6	6	7	316-HT
3	2000	4	6	7	316-HT

### 3.5. Metrology

The surface roughness ( $S_q$ ) of the samples were all evaluated on a scanning white light interferometer. The form error (PV) for the tungsten carbide mould was measured on a multi-wavelength non-contact interferometer. The form error for the silicon carbide and fused silica samples were measured on a PGI Optics profilometer.

Surface finish and form measurements were taken after every fourth machining cut on the tungsten carbide mould. The silicon carbide and fused silica samples were measured after each pass. The details of the metrology equipment and the qualifying metrics can be found in Table 4.

**Table 4** Metrology equipment and metrics

Instrument	Specification	Details
Zygo Nexview NX2	Objective	20 $\times$
	Field of view	434 $\mu\text{m}$ $\times$ 434 $\mu\text{m}$
	Fitting operation	4 <sup>th</sup> order polynomial removed
	Metric	RMS roughness, $S_q$ (nm)
LUPHOScan 420	Fitting operation	Piston, tilt, and power removed
	Metric	Peak-to-valley, PV ( $\mu\text{m}$ )
PGI Optics	Fitting operation	Nominal geometry removed
	Metric	Peak-to-valley, PV ( $\mu\text{m}$ )

## 4. Results and Discussion

### 4.1. Tungsten carbide workpiece results

The tungsten carbide mould was machined until the surface roughness ( $S_q$ ) was below 10 nm threshold to evaluate the

usable cutting distance during SPDT of tungsten carbide. During both tests, it was observed that the RMS roughness exceeded the threshold value of 10 nm after a cutting distance of 1 km. This is shown in Figure 3a and Figure 3b where surface finish obtained from both tests was below the threshold value after tool had covered a cutting distance of 0.5 km. Figure 3c and 3d depicts the surface finish obtained from both tests after tool had covered a cutting distance of 1 km. Figure 4 shows the variation in surface finish over a cutting distance of 0.92 km for Test 1 and Test 2. It was seen that the surface texture degraded over increasing cutting distance. A higher roughness value at the beginning of Test 2, see Figure 4, may be due to subsurface damage from previous test.

The variation in surface form error was also analysed to evaluate the usable cutting distance during SPDT of tungsten carbide mould. It was seen that the surface form remained consistent over the duration of the test and any slight variations in the shape could be attributed to increase in tool wear over increasing cutting distances. Figure 5a and 5b shows the form error obtained from Test 1 and Test 2 after the tool had covered a cutting distance of 0.7 km. Since two different diamond tools of identical geometry were used for these tests, variation in their waviness profile could explain the difference between their PV value.

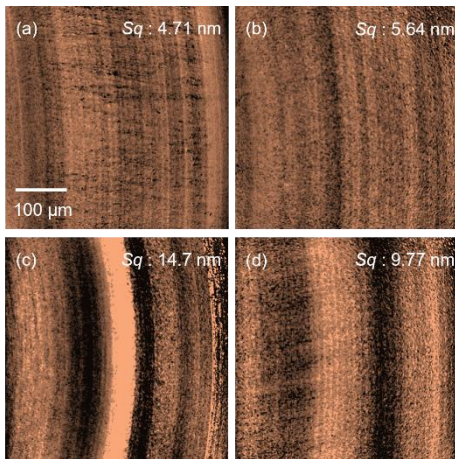


**Figure 3.** Surface maps and RMS roughness near the edge of the WC workpiece a) after cutting distance of 0.5 km during Test 1, b) after cutting distance of 0.5 km during Test 2, c) after cutting distance of 1 km during Test 1, d) after cutting distance of 1 km during Test 2.

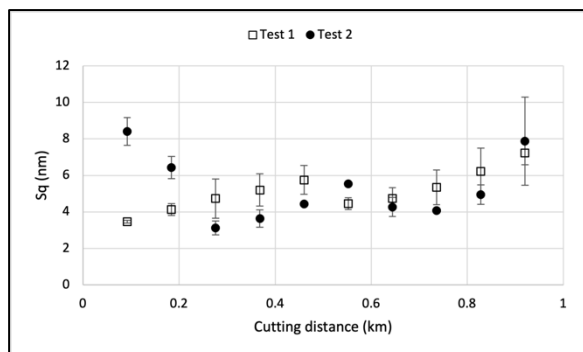


**Figure 4.** Surface finish variation along tool cutting distance for Test 1 and Test 2.

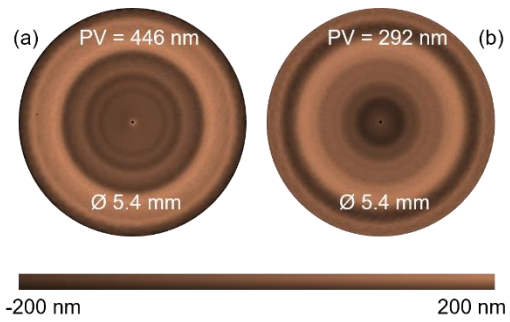


**Figure 5.** Surface form after tool cutting distance of 0.7 km a) Form error for Test 1, b) Form error for Test 2

#### 4.2. Silicon carbide workpiece results

These tests were performed sequentially from test one through three and then the tool was resharpener for test four through five. After each test three surface measurements at three different radii were taken and averaged for each radius position. These zones are labelled center, within 1 mm radius of the center, middle, within 5 mm to 7 mm radius of the center, and the edge, outside the 12 mm radius from the center of the workpiece. The tests are preliminary and because the workpiece was a flat only surface finish data was recorded. The overall results of the tests are shown in Figure 6.

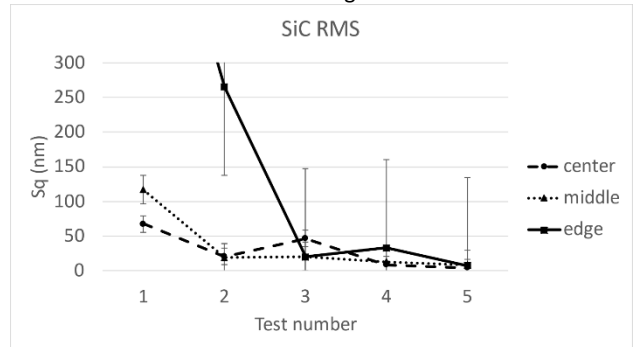


**Figure 6.** RMS roughness of SiC sample. The tool was re-lapped between test 3 and test 4.

It can be seen by the data in Figure 6 that there were significant improvements made to the roughness of the part as the feedrate decreased and as the laser power increased. The surface finish of the best zones of the finished part are shown in Figure 7. The data shown in Figure 7 display both ductile and brittle fracture material removal. The brittle fracture could be due to several factors and more research must be conducted to further investigate this.

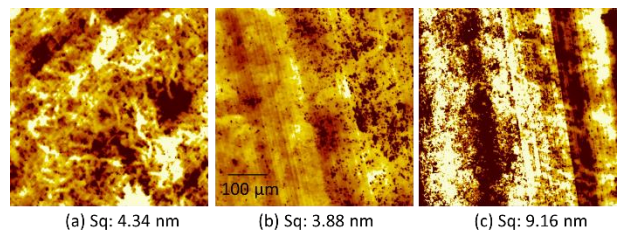


**Figure 7.** Surface of the SiC workpiece a) at the center of the part, b) at the middle of the part, c) at the center of the part

#### 4.3. Fused silica workpiece results

The fused silica sample was machined with various parameters to achieve in combination the best surface and form error with a relatively short cutting time. Table 5 shows the results of the RMS of the surface of the work piece as well as the peak to valley (PV) of the form error for each of the tests.

**Table 5** Fused silica surface roughness

Test No.	Center Sq (nm)	Middle Sq (nm)	Edge Sq (nm)	Form error PV ( $\mu\text{m}$ )
1	29	45	41	0.88
2	45	90	160	1.48
3	23	62	83	0.71

Figure 8 gives a good representation of the uniformity of the surface finish of the fused silica glass workpiece. This is critical because the workpiece would have to be post polished for the final lens but the time taken to post polish the lens is dependant on the worst portion of the workpiece. Figure 9 shows the form errors for the workpiece from test 3 and as expected from a turning operation they are symmetrical.

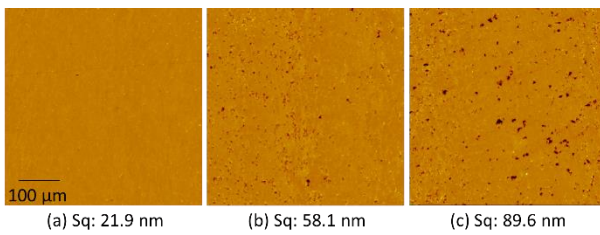


**Figure 8.** Surface of the test 3 fused silica workpiece a) at the center of the part, b) at the middle of the part, c) at the center of the part.

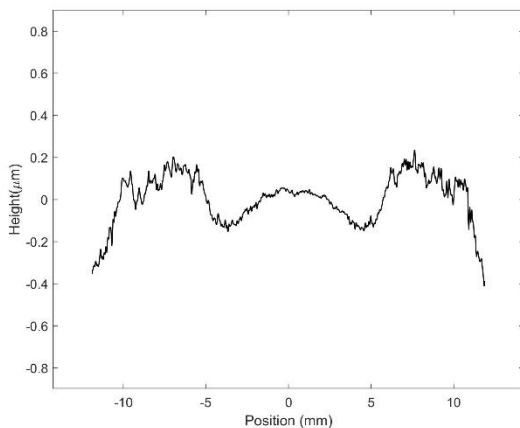


**Figure 9.** Surface of the test 3 fused silica workpiece a) at the center of the part, b) at the middle of the part, c) at the center of the part.

Figure 9 shows promising form error because the symmetrical form errors could be compensated in subsequent cuts. Using corrections form errors have typically been observed in the 350 nm to 500 nm range. This is from tool degradation as the workpiece is cut. Currently, only a few cuts can be performed before the tool has completely failed.

## 5. Conclusion

The summary all three materials, tungsten carbide, silicon carbide, and fused silica, are able to be diamond turned to a point where deterministic polishing time would be significantly reduced. Results for tungsten carbide are promising for the moulding industry with the ability to achieve less than 10 nm for surface roughness with nearly a 1 km track length. As previously stated, the results for silicon carbide are extremely preliminary with only machining a 25 mm flat, but the results are very promising with achieving surfaces below 10 nm as well. The machining of fused silica at this point will need post polishing to achieve an optical level surface roughness but there is some potential for it to reduce polishing times having the ability to achieve reasonable form errors between one to two fringes and

a useable surface finish for polishing. Overall, using the  $\mu$ -LAM system does potentially allow for machining hard and brittle materials as compared with traditional diamond turning.

## References

1. Yin, L., et al., Ultraprecision grinding of tungsten carbide for spherical mirrors. Proceedings of the Institution of Mechanical Engineers, Part B: *Journal of Engineering Manufacture*, 2004. **218**(4): p. 419-429.
2. Feng, G., J. Guo, and G. Zhang, Material removal characteristics of ultra-precision grinding silicon carbide ceramics. *Advances in Applied Ceramics*, 2020. **119**(4): p. 175-182.
3. Hall, C., et al. Magnetorheological Finishing of Tungsten Carbide Mold Materials. in *International Optical Design Conference and Optical Fabrication and Testing*. 2010. Jackson Hole, Wyoming: Optical Society of America.
4. Mishra, V., et al. Development of Tungsten Carbide Mold by Diamond Turning Process. in *OSA Optical Design and Fabrication 2021 (Flat Optics, Freeform, IOFC, OFT)*. 2021. Washington, DC: Optical Society of America.
5. Li, Z., et al., Ultrasonically Assisted Single Point Diamond Turning of Optical Mold of Tungsten Carbide. *Micromachines*, 2018. **9**(2): p. 77.
6. Shahinian, H., et al., Microlaser assisted diamond turning of precision silicon optics. *Optical Engineering*, 2019. **58**(9): p. 1-8, 8.